Effect of variation in contact friction on the performance of the under-platform dampers

26th INTERNATIONAL CONGRESS ON SOUND AND VIBRATION
7-11 July 2019, Montreal

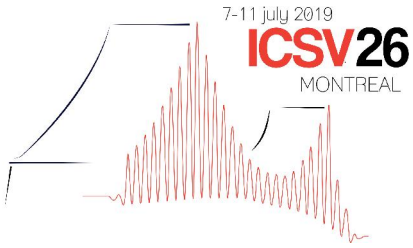

EFFECT OF VARIATION IN CONTACT FRICTION ON THE PERFORMANCE OF THE UNDER-PLATFORM DAMPERS.

Muhammad Umer
Politecnico di Torino, Italy
email: muhammad.umer@polito.it

Daniele Botto
Politecnico di Torino, Italy

Stefano Zucca
Politecnico di Torino, Italy

Under platform-dampers (UPDs) are commonly used devices in turbomachinery to mitigate the turbine blade vibrations caused by the periodically fluctuating stresses. These dampers are placed in the underside of two adjacent blades and vibration energy is partly dissipated by the friction at the blade/damper interfaces. As a result, the vibration amplitude is reduced with beneficial effects on the blade fatigue life. At LAQ AERMEC a novel test rig has been developed to accurately measure the response of a single turbine blade and the kinematics/dynamics of two adjacent UPDs. In this newly developed test rig, each damper is in contact with the under-platform of the blade on one side and with ground/fixed platform on its other side. The dampers are pressed against the blade platform by static forces applied by dead weights. A static force is also radially applied to root of the blade to clamp it to the rig, simulating the effect of the actual centrifugal force in operating conditions. Finally, a transverse periodic excitation is applied in order to excite the blade's first resonances. In this paper, the performance of different UPDs in terms of reduction of the blade vibration amplitude and shift in resonance frequency is studied at two different contact friction conditions (normal and low friction). Low friction conditions are obtained by introducing a thin layer of oil between the damper-blade contact interfaces. Experiments are performed on a real turbine blade to investigate the semi-cylindrical dampers. This profound study of UPDs provides a strong basis to understand the effect of damper with different contact conditions, to limit the blade vibration.

Keywords: under-platform dampers, contact friction, nonlinear vibration

1. Introduction

The complex nature of the forces resulted from the contact friction at the interface between the damper and blade makes the numerical simulation of the damper-blade system quite cumbersome. Therefore, study of the under-platform dampers always involves extensive experimental investigation at various damper-blade loading conditions. The most commonly observed experimental information in this field is the standard Frequency Response Functions (FRFs) of the blade. A number of test rigs [1, 2, 3, 4, 5, 6]

are available which measures the response of the blade for a range of frequencies. These FRFs generally tell us about the overall effect of the damper on the blade in terms of reduction in response amplitude and shift in frequency. However, these FRFs do not provide any information about the insight of the damper contacts. It has been noticed by the researchers [7, 8, 9] that using the FRFs only, as experimental evidence to simulate the damper-blade system, is not a viable practice. This is because the numerical modeling of the damper-blade system requires correct estimation of the contact parameters i.e. contact stiffness and friction coefficient. In this regard, a recently built test rig [10] at LAQ AERMEC[1] has a capability to directly measure the damper contact forces and relative displacements along the tangential direction of the contact interfaces. This test rig also allows to measure the standard frequency response of the blade. In this test rig, a single blade is placed between the two dampers and each damper is in contact with the blade platform on one side whereas on the other touches the ground platform. In this rig, the blade is excited with an electromagnetic shaker attached close to the blade root and the damper static load is applied by the wires and pulleys to simulate the centrifugal load on dampers. The response of the blade is measured by the accelerometer attached at the trailing side of the blade as shown in the top view of the rig in Fig. 1. A through description and working of this novel test bench can be find in [10].

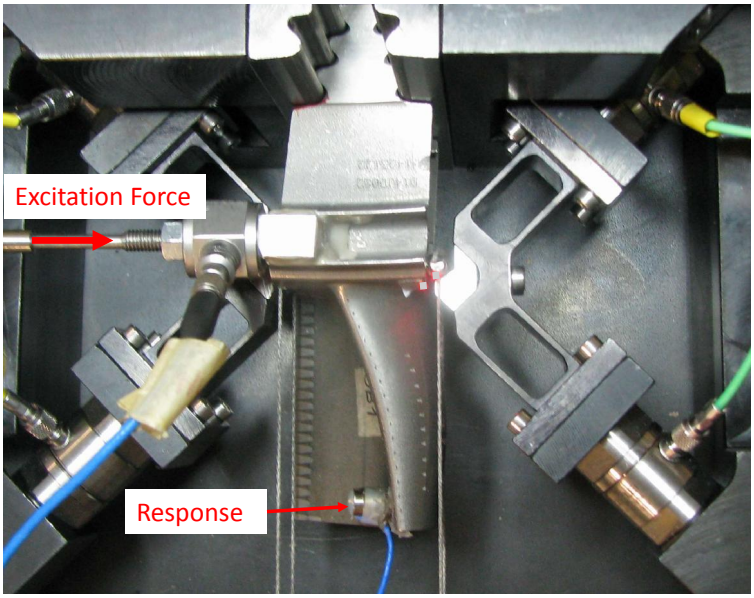

Figure 1: Top view image of the novel test rig with real turbine blade

With refer to the frequency response of the blade, examples of the measured FRFs on this novel test rig with a real blade are given in Fig. 2 at three different levels of the damper static load F_C. It can be observed that under-platform dampers determine significant reduction in the response amplitude of the blade and also result in shift in the blade frequency. Moreover, it can be noticed that the static normal load on the dampers affects both the vibration amplitude and the resonance frequency of the blade. It is quite obvious that higher static load on the dampers causes the increase in normal as well as tangential contact stiffness of the dampers.

Furthermore, from these FRFs it is possible to develop amplitude and frequency damper performance curves which represent the amplitude or frequency shift against the ratio of the damper static load to the blade excitation force. The damper performance curves, namely 'amplitude peak' and 'frequency shift', are produced from the FRFs of the blade [11, 12, 13, 14]. More specifically, the amplitude performance curve plots the maximum amplitude response (displacement, velocity or acceleration) of the

[1] http://www.aermec-dimec.polito.it/

blade against the force ratio F_C/F_E. Whereas, the frequency performance curve plots the shift of the resonance frequency with respect to the same damper static load to excitation force ratio F_C/F_E. Amplitude performance curves are also sometimes called damper optimization curve. The idea of damper performance curves was first introduced by Cameron in [15]. This graphical representation of the experimental data assist the designer to identify a design point for the under-platform dampers independent from the excitation force or viscous damping.

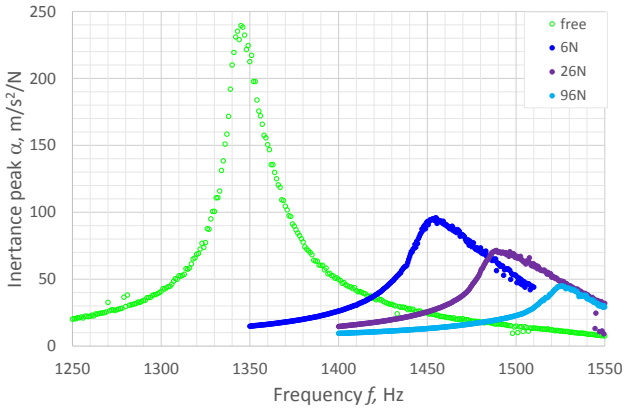

Figure 2: Frequency response of the blade without dampers (free) and with dampers at three different damper static load levels without any oil film

Example of the numerically simulated amplitude and frequency shift damper performance curves are Fig. 4a and 5b, however, a detailed description about numerical contact model and these curves is given in Section 2.

1.1 Objectives

The overall objective of this paper is to experimentally investigate the effect of different friction coefficient on the performance of the dampers. The friction coefficient of the contacts was altered by introducing a thin film of the oil between the both contact interfaces of the damper. In this paper, the experimentally observed variations in the damper performance curves, due to the different friction coefficients, are compared with the simulated damper performance curves obtained by a simple Jenkin contact element.

2. Friction Modeling

One of the most commonly used modeling technique to simulate the frictional contacts is called penalty method. Penalty means that any violation of the contact condition will be punished by generating an opposing contact force. A simple but largely used contact model named Jenkin contact model [16], as shown in Fig. 3 along with its resulting hystesis loop, is based on the penalty method. In this contact model the contact load is determined by the penalty stiffness K_t and the friction coefficient μ. Whereas, in this contact model n_0 corresponds to the normal static load which is practically applied on the dampers with the help of wires and pulleys also denoted here as F_C. While modeling the friction with this contact model, it can be seen from the given four states of the hysteresis loop in Fig. 3b four analytical equations are required. Each side of the hysteresis loop represent different state of the friction force as also

summarized in Table 1. These four equation are actually defined by two constitutive equations as given in Eq. 1 and 2 which differentiate between the stick and slip states of the contact respectively. The Eq. 1 defines the stick state of the contact. This means that at the beginning there is no relative displacement between the ground and slider. In this state the contact behaves linearly and any variation in the friction force is only because of the elastic deformation of the spring. The subscript "*0*" in this Eq.1 refers to the quantities at the beginning of the stick state. As the excitation force further increases, the contact slider reaches to the slip state of the contact which is defined by the coulomb limit as given in 2. In this Eq. 2 of the slip state, "*0*" refers to the constant preload on the contact.

$$f_t = f_0 + k_t(x - x_0) \tag{1}$$

$$f_t = sign(\dot{w})\mu n_0 \tag{2}$$

By applying this Jenkin contact element with SDOF system, the similar damper performance curves as

Table 1: Transition criteria of the contact corresponding to the four states of the friction force

From positive slip to stick (A-B)	$\dot{x}$=0	$\ddot{x}$<0
From stick to negative slip (B-C)	$\|f_t\|>\mu n_0$	$\dot{x}$<0
From negative slip to stick (C-D)	$\dot{x}$=0	$\ddot{x}$>0
From stick to positive slip (B-C)	$\|f_t\|>\mu n_0$	$\dot{x}$>0

explained in Section 1, can be produced. A set of simulated frequency and amplitude damper performance curves are shown in Fig. 4 in which different states of the contact are marked. At a larger value of force ratio F_C/F_E, the contact remains stick and the slider does not move thus non relative displacement between the contact surfaces occur. As we increase the excitation force F_E for a given static normal load on the slider F_C or *n0* the contact starts sliding thus a relative displacement occur. The response amplitude of the structure reduces gradually with increases in excitation force until it reaches to the minimum level. After that point, a further increase in excitation level results in abrupt increase in the response amplitude and it approaches to the free response of the structure. Experimentally, the damper performance curves are measured on the test rig for three different static normal load levels on the dampers as shown in Fig. 5. It can be seen that at higher static load levels on the damper, the response amplitude of the blade is always lower and shift in the frequency level is higher. This trend is consistent with the behavior observed by the FRFs shown in Fig. 2.

3. FRFs Comparison

This section compares the FRFs of the blade with and without oil film at two different damper static load levels. The FRFs of the blade at two different damper static load levels F_C=2kg and 5kg are measured for both cases i.e. with and without oil films between the damper contact interfaces. As shown in Fig. 7, for the damper contact equipped with the oil film, the amplitude and frequency of the blade are lower at both damper static load levels. This variation in the FRFs due to change in the friction coefficient by introducing oil film between the contacts is further investigated by measuring a number of FRFs to develop damper performance curves.

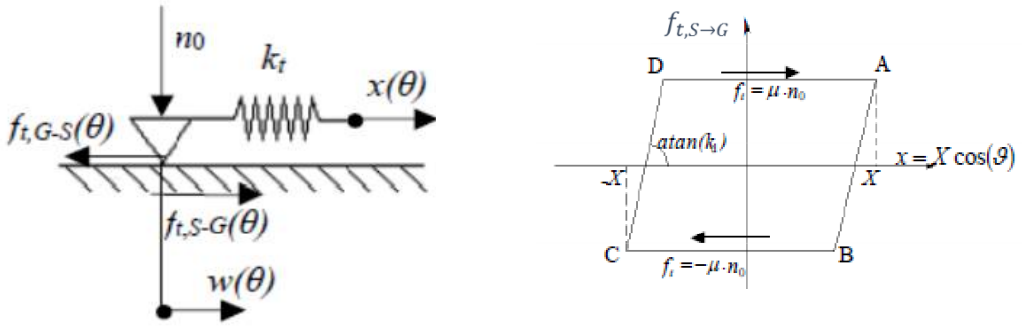

(a) Jenkin contact model with constant normal load

(b) Hysteresis loop developed between the friction force and relative displacement between contact surfaces

Figure 3: 1D friction contact model with its corresponding hysteresis loop

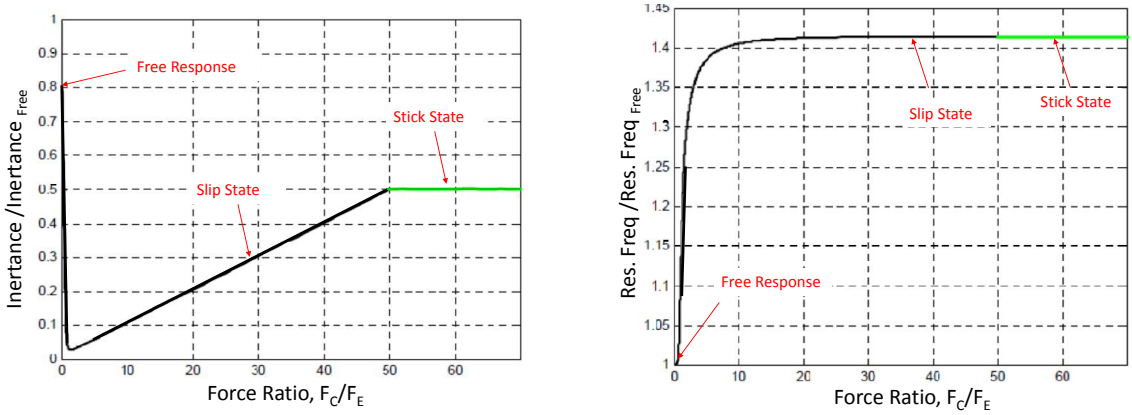

(a) Normalized inertance peak as a function of the force ratio F_C/F_E

(b) Normalized resonance frequency as a function of the force ratio F_C/F_E

Figure 4: Simulated damper performance curves with respect to amplitude and frequency shift

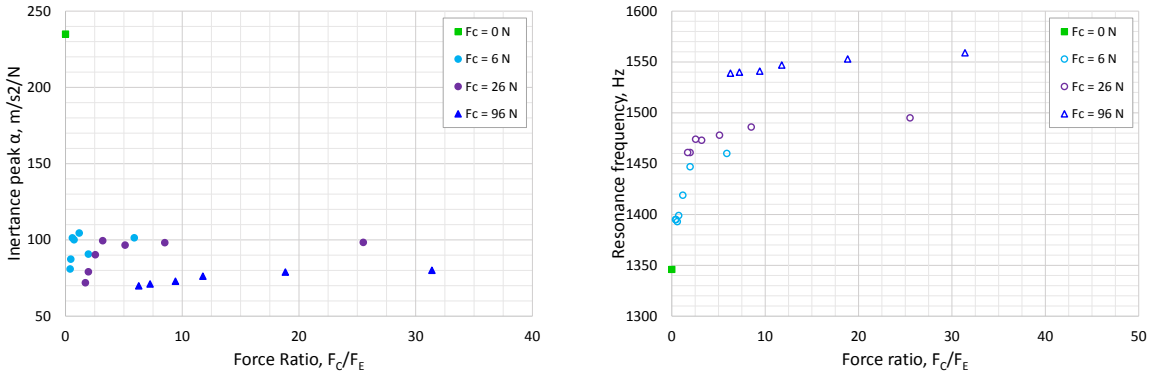

(a) Inertance peak as a function of the force ratio F_C/F_E

(b) Resonance frequency as a function of the force ratio F_C/F_E

Figure 5: Measured damper performance curves with respect to amplitude and frequency shift at three different damper static load levels F_C

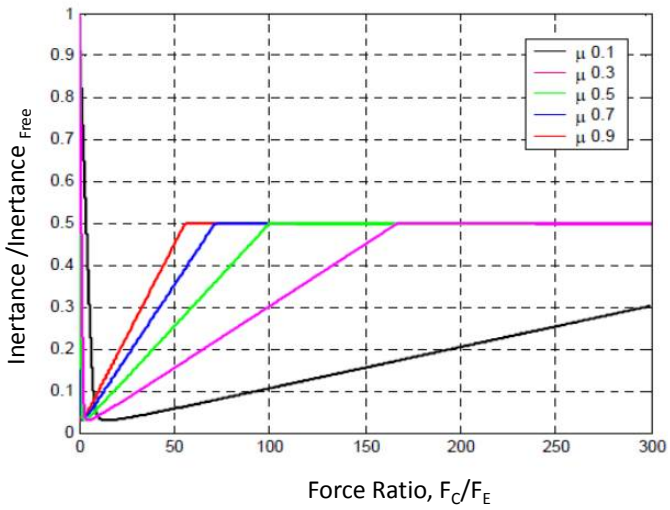

Figure 6: Simulated results of the normalized resonance frequency as a function of the force ratio F_C/F_E for different friction coefficient values μ

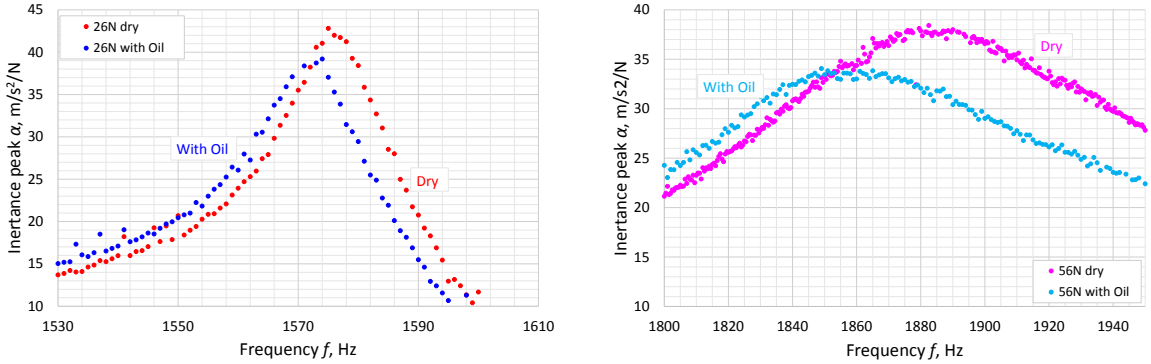

(a) FRFs of the blade with dry and oil filmed contacts at F_C=26N

(b) FRFs of the blade with dry and oil filmed contacts at F_C=56N

Figure 7: Measured frequency response functions of the blade at two different static load levels F_C on the dampers

4. Damper Performance Curves Comparison

In this section, a comparison of the damper performance curves at different friction coefficient is presented. From the numerical point of view, if we further simulate the contact as described in 2, by varying the coefficient of friction, it can be seen that the level of the amplitude performance curves increases with the increase in friction coefficient value as shown in 6. Furthermore, it can also be observed that the stick region of the contact also increases with the friction coefficient μ which is consistent with the fact that higher excitation force (in other words lower force ratio F_C/F_E) is required to surpass the limiting friction value. A quite similar trend has been observed experimentally also (see Fig. 6) in which two different static load levels on the dampers are investigated. It can be seen that in case of no oil film between the contact surfaces, the level of the amplitude performance curves is always higher than without oil film for both damper static load levels. Although in both cases, the response amplitude of the blade reduces with increase in excitation force.

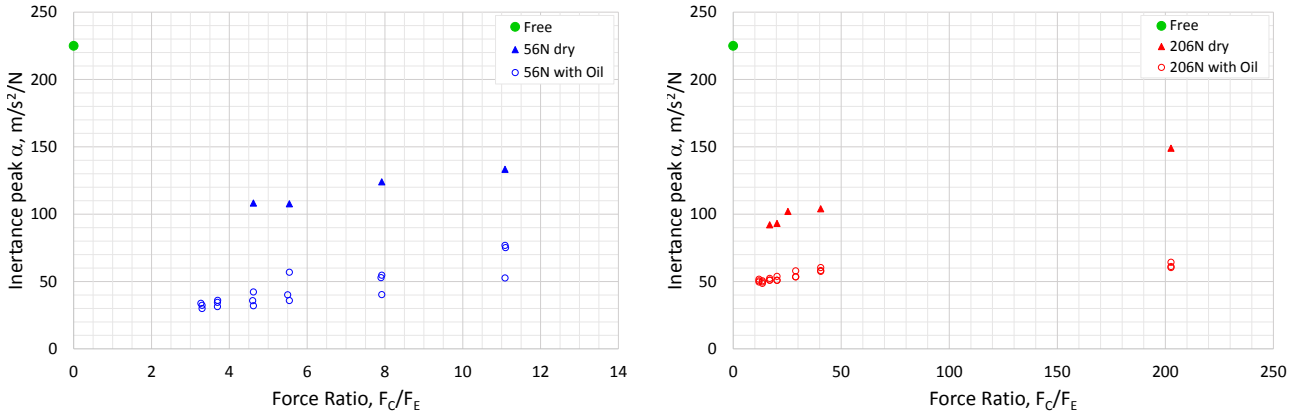

(a) Normalized blade inertance as a function of the force ratio F_C/F_E for static centrifugal load F_C=56N

(b) Normalized blade inertance as a function of the force ratio F_C/F_E for static centrifugal load F_C=206N

Figure 8: Variation in amplitude damper performance curves due to change in friction coefficient

5. Conclusions

In the modeling of the frictional contacts of the damper-blade system, it has already been established that the change in friction coefficient significantly effects the performance of the damper. An exclusive experimental campaign has been carried out to experimentally observe this effect. In this paper, it was found that the performance of the damper has been improved by introducing the oil film between the contact interfaces. It was also observed that the frequency response of the blade is lower in amplitude and frequency for the contacts with oil film compared to the dry contacts. Similarly, the amplitude performance curves of the damper are plotted from the measured FRFs and it has been found that the level of the performance curves in case of low friction (with oil film) is always higher than the higher friction case (dry contacts). This behavior is quite consistent with the numerically simulated behavior of the frictional contacts with the help of simple Jenkin contact model.

REFERENCES

1. Griffin, J. H. Friction damping of resonant stresses in gas turbine engine airfoils, *Journal of Engineering for Power*, **102** (2), 329–333, (1980).

2. Sanliturk, K. Y., Ewins, D. J. and Stanbridge, A. B. Underplatform dampers for turbine blades: theoretical modelling, analysis and comparison with experimental data, *ASME 1999 international gas turbine and aeroengine congress and exhibition*, pp. V004T03A037–V004T03A037, American Society of Mechanical Engineers, (1999).

3. Szwedowicz, J., Kissel, M., Ravindra, B. and Kellerer, R. Estimation of contact stiffness and its role in the design of a friction damper, *ASME Turbo Expo 2001: Power for Land, Sea, and Air*, pp. V004T03A049–V004T03A049, American Society of Mechanical Engineers, (2001).

4. Cigeroglu, E., An, N. and Menq, C. H. Forced response prediction of constrained and unconstrained structures coupled through frictional contacts, *J. Eng. Gas. Turbines Power-Trans. ASME*, **131** (2), 022505–022505–11, (2009).

5. Sever, I. A., Petrov, E. P. and Ewins, D. J. Experimental and numerical investigation of rotating bladed disk forced response using underplatform friction dampers, *J. Eng. Gas. Turbines Power-Trans. ASME*, **130** (4), 042503–11, (2008).

6. Sextro, W., Popp, K. and Wolter, I. Improved reliability of bladed disks due to friction dampers, *ASME Turbo Expo: Power for Land, Sea, and Air*, Orlando, Florida, USA, vol. 4: Manufacturing Materials and Metallurgy; Ceramics; Structures and Dynamics; Controls, Diagnostics and Instrumentation; Education, p. V004T14A035, (1997).

7. Firrone, C. Measurement of the kinematics of two underplatform dampers with different geometry and comparison with numerical simulation, *J. Sound Vibr.*, **323**, 313–333, (2009).

8. Gola, M. M. and Gastaldi, C. Understanding complexities in underplatform damper mechanics, *ASME Turbo Expo 2014: Turbine Technical Conference and Exposition*, pp. V07AT34A002–V07AT34A002, American Society of Mechanical Engineers, (2014).

9. Gola, M. M., Bragas dos Santos, M. and Liu, T. Measurement of the scatter of underplatform damper hysteresis cycle: experimental approach, *ASME International Design Engineering Technical Conferences and Computers and Information in Engineering Conference*, vol. 1, pp. 359–369, (2012).

10. Botto, D. and Umer, M. A novel test rig to investigate under-platform damper dynamics, *Mech. Syst. Signal Proc.*, **100**, 344–359, (2018).

11. Csaba, G. and Andersson, M. Optimization of friction damper weight, simulation and experiments, *Turbo Expo: Power for Land, Sea, and Air*, Florida, USA, vol. 4, p. V004T14A031, (1997).

12. Botto, D., Zucca, S., Pavone, S. and Gola, M. Parametric study of the kinematic behaviour of the underplatform damper and correlation with experimental data, *International Conference on Noise and Vibration Engineering ISMA 2008*, Leuven-Belgium, (2008).

13. Zucca, S., Berruti, T. and Cosi, L. Experimental and numerical investigations on the dynamic response of turbine blades with tip pin dampers, *Journal of physics. Conference Series*, **744** (1), (2016).

14. Gastaldi, C. and Berruti, T. M. A method to solve the efficiency-accuracy trade-off of multi-harmonic balance calculation of structures with friction contacts, *International Journal of Non-Linear Mechanics*, **92**, 25–40, (2017).

15. Cameron, T. M., Griffin, J. H., Kielb, R. E. and Hoosac, T. M. An integrated approach for friction damper design, *Journal of Vibration and Acoustics*, **112** (2), 175–182, (1990).

16. Firrone, C. M. and Zucca, S., (2011), *Numerical Analysis-Theory and Application*, chap. Modelling Friction Contacts in Structural Dynamics and its Application to Turbine Bladed Disks, pp. 301–334. InTech.